The type of article: Research paper

Title: Global patterns and drivers of leaf photosynthetic capacity: the relative importance of environmental factors and evolutionary history

Running title: Drivers of global photosynthetic capacity

Zhengbing Yan, Jordi Sardans, Josep Peñuelas, Matteo Detto, Nicholas G. Smith, Han Wang, Lulu Guo, Alice C. Hughes, Zhengfei Guo, Calvin K. F. Lee, Lingli Liu, Jin Wu

Abstract

Aim: Understanding the considerable variability and drivers of global leaf photosynthetic capacity (indicated by the maximum carboxylation rate standardized to 25°C; $V_{c,max25}$) is an essential step for accurately modelling terrestrial plant photosynthesis and carbon uptake under climate change. Although current environmental conditions have often been connected with empirical and theoretical models to explain global $V_{c,max25}$ variability through acclimation and adaptation, long-term evolutionary history has largely been neglected, but may also explicitly play a role in shaping the $V_{c,max25}$ variability.

Location: Global

Time period: Contemporary.

Major taxa studies: Terrestrial plants

Methods: We compiled a geographically comprehensive global dataset of $V_{c,max25}$ for C_3 plants (n= 6917 observations from 2157 species and 425 sites covering all major biomes worldwide), explored the biogeographic and phylogenetic patterns of $V_{c,max25}$, and quantified the relative

importance of current environmental factors and evolutionary history in driving global $V_{c,max25}$ variability.

Results: We found that $V_{c,max25}$ differed across different biomes with higher mean values in relatively drier regions, and across different life-forms with higher mean values in non-woody relative to woody plants and in legumes relative to non-leguminous plants. $V_{c,max25}$ displayed a significant phylogenetic signal and diverged contrastingly across phylogenetic groups, with a significant trend along the evolutionary axis towards the higher $V_{c,max25}$ in more modern clades. A Bayesian phylogenetic linear mixed model revealed that evolutionary history (indicated by phylogeny and species) explained nearly three-fold more of the variation in global $V_{c,max25}$ than present-day environment (53% vs 18%).

Main conclusions: These findings contribute to a comprehensive assessment of the patterns and drivers of global $V_{c,max25}$ variability, highlighting the importance of evolutionary history in driving global $V_{c,max25}$ variability and, resultingly, terrestrial plant photosynthesis.

Keywords: biogeography, biome, environmental factor, evolutionary history, global carbon cycling, life-form, photosynthetic capacity, phylogeny, species

1 Introduction

Accurate predictions of terrestrial ecosystem responses to global environmental changes require correct modelling of land plant photosynthesis in terrestrial biosphere models (TBMs), the largest carbon flux in the global carbon cycle (Bonan & Doney, 2018; Walker et al., 2021). The amount of carbon assimilated by land plants depends on the interactions between external environmental factors and the intrinsic photosynthetic machinery, which is primarily controlled by the maximum carboxylation rate of the enzyme Ribulose-1,5-bisphosphate carboxylase/oxygenase (RuBisCO) in the chloroplasts ($V_{c,max}$; Rogers et al., 2017). Given that RuBisCO has reached an evolutionary trapped state suggested by limited variation in its catalytic activity among phylogenetically distant clades (Bracher et al., 2017), $V_{c,max25}$ ($V_{c,max}$ standardized to a reference temperature of 25℃) mainly reflects the amount of RuBisCO enzyme present per leaf area, and directly mediates biotic regulations of photosynthetic carbon uptake and interactions with climate from individual plants to large, vegetated landscapes. It is also a key parameter at the heart of many photosynthetic schemes in TBMs (Farquhar et al., 1980; Kattge et al., 2009; Bernacchi et al., 2013; Wu et al., 2016; Wang et al., 2020). Despite its importance, however, $V_{c,max25}$ is highly dynamic in nature, and is influenced by multiple abiotic and biotic factors, such as climate conditions, soil variables, and species properties (Kattge et al., 2009; Walker et al., 2014; Ali et al., 2015; Smith & Dukes, 2018; Detto & Xu, 2020). Accurate characterization and understanding of $V_{c,max25}$ variability thus represent a fundamental step for improving the modelling of plant photosynthesis in TBMs (Rogers et al., 2017; Bonan & Doney, 2018). Although understanding and predicting $V_{c,max25}$ variability have received much scientific attention (Kattge et al., 2009; Ali et al., 2016; Smith et al., 2019; Peng et al., 2021), a holistic understanding and assessment of the patterns and drivers of global $V_{c,max25}$ variability is still needed.

Current environmental conditions have been assimilated into both empirical and theory-based optimality models for interpreting the large-scale $V_{c,max25}$ variability (Prentice et al., 2014; Ali et al., 2016; Smith et al., 2019; Peng et al., 2021). For example, studies have revealed associations between $V_{c,max25}$ and present-day temperature, water, light, soil pH and soil nutrients they are subjected to across large geographical extents (Paillassa et al., 2020; Peng et al., 2021; Luo et al., 2021). The likely underlying reason is that these environmental factors mediate plant photosynthetic carbon gain and water or nutrient costs for the construction of RuBisCO, and thus determine plant investment in $V_{c,max25}$ (Prentice et al., 2014; Paillassa et al., 2020; Wang et al., 2020). These empirical observations motivated subsequent theoretical explorations of $V_{c,max25}$ variability relying on environmental factors, such as the eco-evolutionary optimality theory that establishes that plants optimize their $V_{c,max25}$ to best adapt to their living environment to maximize photosynthetic carbon gain (Ali et al., 2016; Smith et al., 2019; Jiang et al., 2020). Moreover, environmental factors could affect $V_{c,max25}$ variability indirectly by filtering species occurrences and driving biotic competition among species, which in turn feeds back to plant nitrogen (N) uptake and other processes related to plant photosynthesis (Kattge et al., 2009; Smith & Dukes, 2018). Through these processes, $V_{c,max25}$ has been found to differ considerably across vegetated biomes and life-forms (Kattge et al., 2009; Ali et al., 2015; Smith & Dukes, 2018; Luo et al., 2021). Despite recent progress in elucidating the patterns and factors responsible for large-scale $V_{c,max25}$ variability, current environmental conditions are generally considered as the major independent variables to explain global site-mean $V_{c,max25}$ variability, with the predictive power often found to be low to moderate (Ali et al., 2016; Smith et al., 2019; Peng et al., 2021; Luo et al., 2021). Thus,

84 whether other factors related to plants themselves also play an important role in shaping the large-
85 scale $V_{c,max25}$ variability remains unclear.
86
87 One candidate, yet underexplored, factor of $V_{c,max25}$ variability is evolutionary history of plants,
88 the complex and long-term product of evolutionary processes resulting from natural selection over
89 time (Cavender-Bares et al., 2016; Peñuelas et al., 2019; Sardans et al., 2021). These evolutionary
90 processes according to the timescale can be simplified by phylogeny and species. The phylogenetic
91 term accounts for the variability in shared ancestry (i.e., the ancient adaptation and differentiation
92 from other clades), while the species term accounts for the interspecific variability independent of
93 the shared ancestry, mostly due to recent processes of evolutionary convergence and divergence
94 not yet incorporated to the long-term evolutionary separation among taxonomic clades (Sardans et
95 al., 2021; Vallicrosa et al., 2022a). The evolutionary history, together with current environmental
96 conditions, have contributed to the distribution of modern biomes (Cavender-Bares et al., 2016),
97 and can leave an imprint on plant photosynthetic traits, such as the maximum leaf photosynthetic
98 rate (Gago et al., 2019; Flexas & Carriquí, 2020; Huang et al., 2022; Liu et al., 2022). Meanwhile,
99 evolutionary history has been demonstrated to explain 84-94% of the large-scale variability in leaf
100 nitrogen (N) and phosphorus (P) concentrations (Sardans et al., 2021; Vallicrosa et al., 2022a,b),
101 both of which are essential components of RuBisCO enzyme and directly correlate with $V_{c,max25}$
102 (Walker et al., 2014; Bahar et al., 2017). Also, there is empirical evidence that genotypes and
103 phylogeny can alter RuBisCO kinetic parameters (Jump & Peñuelas, 2005; Galmes et al., 2015).
104 All together, these accumulated clues suggest that evolutionary history may be a key and
105 fundamental factor in driving the global variability in $V_{c,max25}$, but the phylogenetic structure of

$V_{c,max25}$ and the relative importance of current environmental factors and evolutionary history in shaping the $V_{c,max25}$ variability on a global scale remain largely unknown.

The aim of this study is to explore biogeographic patterns and phylogenetic structure of $V_{c,max25}$ on a global scale, and to comprehensively assess the relative roles of current environmental factors and long-term evolutionary history in explaining the global $V_{c,max25}$ variability. Specifically, we ask the following three questions: (1) What are the patterns of $V_{c,max25}$ varying across vegetated biomes and life forms? (2) Does $V_{c,max25}$ have a phylogenetic signal and vary across phylogenetic groups? (3) What is the relative importance of environmental factors and evolutionary history in shaping global $V_{c,max25}$ variability? We address these questions by testing the following hypotheses: (1) $V_{c,max25}$ could vary across different vegetated biomes and life forms, with the relatively higher values in grasslands relative to shrublands and forests, and in fast-growing relative to slow-growing species, because the former plant types usually have higher nutrient concentrations that often are related to more investments in photosynthetic apparatus (Kattge et al., 2009; Ali et al., 2016; Smith & Dukes, 2018); (2) $V_{c,max25}$ shows a significant phylogenetic signal as Vc,max25 has been previously connected with multiple biotic factors (i.e. RuBisCO kinetic parameters and photosynthesis-associated leaf nutrient concentrations) that all display strong phylogenetic regulation (Jump and Peñuelas, 2005; Galmes *et al.*, 2015; Sardans *et al.*, 2021; Huang *et al.*, 2022; Liu *et al.*, 2022); and (3) the global patterns of $V_{c,max25}$ are jointly regulated by both current environmental factors and long-term evolutionary history, with the latter being the dominant driver, because mounting evidence suggests more important contribution of species identity information to the variability of photosynthesis-associated leaf nutrient concentrations than environmental factors (Dahlin *et al.*, 2013; Asner *et al.*, 2014; Sardans *et al.*,

2021; Palacio *et al.*, 2022; Vallicrosa *et al.*, 2022a,b). To test these three hypotheses, we first collated a global dataset of field measured $V_{c,max25}$ for C_3 plants with concurrent measurements of present-day environmental factors (i.e., climate and soil variables), and then integrated this unique global dataset with multiple statistical modelling analyses detailed below.

2 Materials and Methods

2.1 Field dataset of $V_{c,max25}$, climate and soil variables

A geographically comprehensive global dataset of $V_{c,max25}$ for C_3 plants was compiled from three different sources, including one data record from three contrasting forest ecosystems in China (Yan et al., 2021), and two global datasets compiled by Smith et al. (2019) and Peng et al. (2021), respectively. The two global datasets were mainly derived from earlier compilations from different authors or open data sources, including Atkin et al. (2015), Bahar et al. (2017), Bloomfield et al. (2018), Cernusak et al. (2011), Domingues et al. (2010, 2015), Dong et al. (2017), Maire et al. (2015), Meir et al. (2007), Smith & Dukes (2017), Walker et al. (2014), Wang et al. (2018), Xu et al. (2021), and the TRY plant trait database (https://www.try-db.org/TryWeb/dp.php). In this newly compiled global $V_{c,max}$ dataset, we only retained records with concurrent measurements of leaf temperature. With $V_{c,max}$ derived at its measurement temperature (T_{obs}, ℃), or $V_{c,maxTobs}$, we then calculated $V_{c,max}$ at 25℃ ($V_{c,max25}$), using a modified Arrhenius function (Equations 1-2) that describes the instantaneous response of enzyme kinetics to any given temperature (Kattge et al., 2007).

$$V_{c,\mathrm{max25}} = V_{c,\mathrm{maxT_{obs}}} \times f(T_{obs}, 25) \quad (1)$$

where

$$f(T_{obs}, 25) = e^{\frac{H_a(25-T_{obs})}{298.15R(T_{obs}+273.15)}} \times \frac{1+e^{\frac{(T_{obs}+273.15)\Delta S - H_d}{R(T_{obs}+273.15)}}}{1+e^{\frac{298.15\Delta S - H_d}{298.15R}}} \quad (2)$$

where H_d is the deactivation energy (200,000 J mol^{-1}), H_a is the activation energy (71,513 J mol^{-1}), R is the universal gas constant (8.314 J mol^{-1} K^{-1}), and ΔS is an entropy term (J mol^{-1} K^{-1}) calculated following Kattge & Knorr (2007):

$$\Delta S = -1.07 \times T_g + 668.39 \quad (3)$$

Where T_g is the mean growing-season temperature as defined below. All the records in this dataset were reported to be measured from natural vegetation, with 6917 measurements from 2157 species and 425 sites covering all major biomes worldwide (Fig. 1). In addition, all these $V_{c,max}$ measurements were accompanied with corresponding records of present-day climate and soil variables.

Our dataset had six climate variables, including temperature, precipitation, incoming photosynthetically active radiation (PAR), vapor pressure deficit (VPD), atmosphere CO_2 concentration (C_a) and elevation (indicator of atmospheric pressure). We chose these six climate variables due to their empirical or theoretical links to $V_{c,max25}$ variability as explored previously (Ali et al., 2015; Smith & Dukes, 2018; Smith et al., 2019; Jiang et al., 2020; Peng et al., 2021). Specifically, at each site, temperature, precipitation, PAR and VPD were calculated using the average values across the full growing season, which was defined as all the months with mean monthly air temperature above 0 ℃. These four climate variables were extracted using the corresponding coordinates of each site from monthly, 1901-2015, 0.5° resolution data provided by the Climatic Research Unit (CRU TS4.01) climatology data (Harris et al., 2014). C_a was mostly extracted from original records in the databases but was approximated using the corresponding value from global average estimates by the NASA GISS model (https://data.giss.nasa.gov/modelforce/ghgases/) when C_a records were lacking in some cases.

Elevation was mostly extracted from original records in the databases but was estimated using the extracted values from 0.5° resolution data from the WFDEI meteorological forcing dataset (Weedon et al., 2014) when elevation records were lacking in some cases. Temperature and precipitation were three-dimensionally interpolated to the actual site locations (i.e., latitude, longitude, and elevation) using Geographically Weighted Regression following Peng et al. (2021), while PAR and VPD were calibrated to the site-specific elevation following Smith et al. (2019).

In addition, our dataset had ten soil variables, including carbon (C) concentration, nitrogen (N) concentration, C:N ratio, cation exchange capacity (CEC), silt concentration, clay concentration, sand concentration, bulk density, pH, and the ratio of actual evapotranspiration to equilibrium evapotranspiration (Priestley-Taylor coefficient, α) as an indicator of plant-available surface moisture. These ten variables comprehensively reflected soil physical and chemical properties and were chosen primarily due to their apparent correlations with large-scale variability in plant photosynthetic traits (Prentice et al., 2014; Maire et al., 2015; Smith et al., 2019; Paillassa et al., 2020; Peng et al., 2021). α of each site was calculated at the 0.5° resolution with the SPLASH model run at a monthly timescale (Davis et al., 2017). Other soil variables were extracted using the corresponding coordinates of each site from a 250-m resolution global data at the top 30 cm depth provided by the ISRIC SoilGrids database (https://soilgrids.org/).

2.2 Classification of the types of biomes and life-forms

To explore the biogeographic patterns of global $V_{c,mx25}$ variability, we analysed the variability of $V_{c,max25}$ across different biomes. Following the criteria of classic Whittaker Biome Classification system based on mean annual precipitation and mean annual temperature (Whittaker, 1975), all

198 our study sites were grouped into nine biomes: tundra, boreal forest, temperate seasonal forest,
199 temperate rainforest, tropical rainforest, tropical seasonal forest/savanna, subtropical desert,
200 temperate grassland/desert, and woodland/shrubland.
201
202 To explore the change in $V_{c,max25}$ across different life-forms, we first verified the scientific names
203 of each species against The World Checklist of Vascular Plants
204 (https://www.gbif.org/dataset/f382f0ce-323a-4091-bb9f-add557f3a9a2) and The Leipzig
205 Catalogue of Vascular Plants (https://idiv-biodiversity.github.io/lcvplants/), and identified the
206 plant functional group for each species according to the following literature: the TRY plant trait
207 database (https://www.try-db.org/TryWeb/Home.php), the Flora of China (http://frps.eflora.cn/),
208 Useful Tropical Plants (http://tropical.theferns.info/), Australian Native Plants
209 (https://www.anbg.gov.au/index.html), and Wikipedia (https://en.wikipedia.org/wiki). Afterwards,
210 we categorized species into woody or non-woody (i.e., herbaceous) species, and legume or non-
211 leguminous plants. The woody species were further categorized into broadleaved or coniferous
212 species, and evergreen or deciduous species, while the non-woody species were further categorized
213 into perennial (including biennial species) or annual species, and forb or graminoid species.
214
215 **2.3 Statistical analysis**
216 All the statistical analyses were conducted upon the R code (see Method S1 for details).
217 **2.3.1 Cross-comparison of $V_{c,max25}$ variability across different biomes and life-forms**
218 Following Han et al. (2005), we characterized the biogeographic patterns of $V_{c,max25}$ across
219 different biomes using data at the site-species level (i.e., the averaged $V_{c,max25}$ for each species
220 within the same sampling site), and explored the change in $V_{c,max25}$ across different life-forms using

data at the species level (i.e., the averaged $V_{c,max25}$ for each species). We assessed the normality of the $V_{c,max25}$ distribution with the Shapiro-Wilk test using the software platform R 4.0.5 (R Development Core Team, 2021) and found that a log-transformation improved the normality of $V_{c,max25}$. Therefore, differences among different biomes or life-forms for the log transformed $V_{c,max25}$ were determined using one-way analysis of variance (ANOVA) with the least significant difference post-hoc test.

2.3.2 Phylogenetic analysis of $V_{c,max25}$

To characterize the phylogenetic structure of $V_{c,max25}$, two levels of analyses were conducted at the species level. First, we calculated the phylogenetic signal (i.e., Pagel's λ), which indicates the strength of trait convergence within lineages resulting from stabilizing selection, and environmental constraints (Münkemüller et al., 2012). A phylogenetic tree was constructed using the R package 'V.PhyloMaker' based on an available mega-phylogeny of vascular plants (Jin & Qian, 2019). We calculated Pagel's λ using the phylosig function from the R package 'phytools' based on the variance in phylogenetically independent contrasts relative to tip shuffling randomization (Revell, 2012). We chose the Pagel's λ as the phylogenetic signal because it can discriminate between complex models of trait evolution and provide a reliable measurement of effect size (Münkemüller et al., 2012). In addition, Pagel's λ is not sensitive to the number of species in the phylogeny and suitable for large phylogenies with >50 species (or taxa) (Felsenstein, 1985). Second, we cross-compared the variability in $V_{c,max25}$ among different phylogenetic groups. Species were divided into five phylogenetic groups including pteridophyte, gymnosperm, magnoliids, monocotyledon and dicotyledon, following the evolutionary time from the oldest to the youngest (Zhang et al., 2020).

2.3.3 Disentangling the relative contribution of environmental factors and evolutionary history to global $V_{c,max25}$ variability

To explore the separate and joint effects of current environmental factors and evolutionary history on global $V_{c,max25}$ variability, we performed two analyses at the site-species level, in which the averaged $V_{c,max25}$ for each species within the same sampling site was used. In the first analysis, we quantified the effects of current environmental factors as a whole on the $V_{c,max25}$ variability, and identified the most important variables. To reduce the impact of multicollinearity among the environmental factors (Fig. S1), we retained only the variables with correlation coefficients having absolute values below 0.7 and variance inflation factor (VIF) below 10 (Doetterl et al., 2015; Table S1). We then used the R package 'glmulti' to perform the model selection for $V_{c,max25}$ based on the corrected Akaike Information Criterion (AICc) and evaluated the relative importance of each environmental variable based on the sum of the Akaike weights for the models in which the variable was included. A cut-off relative importance value of 0.8 was set to differentiate between the important and unimportant variables (Du et al., 2020). We further conducted partial regression plots to illustrate the effect sign (positive or negative) of each selected variable on $V_{c,max25}$ variability while holding all the other variables constant at their median values, using the R package 'visreg' under the 'conditional plot' scenario (Calcagno & de Mazancourt, 2010; Breheny & Burchett, 2017; Du et al., 2020).

In the second analysis, we used a Bayesian phylogenetic linear mixed model from the R package 'MCMCglmm' to disentangle the relative contributions of current environmental factors and evolutionary history to the global $V_{c,max25}$ variability. We selected only the most important

environmental factors identified above as fixed factors and the phylogeny and species as random factors. For the phylogeny, we used the phylogenetic tree constructed in section 2.2 based on an available mega-phylogeny of vascular plants (Jin & Qian, 2019). The random factors described the effect of evolutionary history on $V_{c,max25}$ variability, with the phylogenetic term accounting for the variability in shared ancestry, and the species term accounting for the interspecific variability independent of the shared ancestry (Sardans et al., 2021; Vallicrosa et al., 2022a,b). To examine whether intraspecific variability would affect the Bayesian phylogenetic linear mixed model performance, we performed a sensitivity analysis on the model that respectively was conducted at individual level (i.e., all original data of $V_{c,max25}$ from individual observations) or site-species level (i.e., the averaged $V_{c,max25}$ for each species within the same sampling site). Our sensitivity analysis demonstrated that the results remained consistent regardless of the analysis at individual or site-species level (Table S5). For clarity, we primarily focused on presenting the data analysis for the Bayesian phylogenetic linear mixed model at site-species level thereafter.

3 Results

3.1 Patterns of $V_{c,max25}$ across biomes and life-forms

To investigate the biogeographical patterns of $V_{c,max25}$, we cross-compared the $V_{c,max25}$ variability across different Whittaker biomes and life-forms. Our results showed that $V_{c,max25}$ varied considerably across biomes, with the mean values maximum in the subtropical desert and temperate grassland/desert, minimum in the tropical and temperate rainforests, and intermediate in other biomes (i.e., boreal forest, tropical seasonal forest/savanna, tundra, temperate seasonal forest and woodland/shrubland) (Fig. 2a; Table S1). We further observed large $V_{c,max25}$ variability across life-forms, with higher $V_{c,max25}$ values in non-woody relative to woody plants, and in legume

relative to non-legume plants (Fig. 2b and 2c; Table S2). Dividing the woody plants into sub-categories, we found that deciduous relative to evergreen plants had higher $V_{c,max25}$, while broadleaved and coniferous plants had no significant difference in $V_{c,max25}$ (Fig. 2d and 2e; Table S2). Dividing the non-woody plants into sub-categories, we found that annuals relative to perennials had significantly higher $V_{c,max25}$, while forb and grass had no significant difference in $V_{c,max25}$ (Fig. 2f and 2g; Table S2). Importantly, whilst the differences in $V_{c,max25}$ means were sometimes quite large, there was considerable overlap between the $V_{c,max25}$ ranges across biomes and life-forms.

3.2 Phylogenetic structure of $V_{c,max25}$

To investigate the phylogenetic structure of $V_{c,max25}$, we analysed the phylogenetic signal of $V_{c,max25}$, and cross-compared the variation in $V_{c,max25}$ across different phylogenetic groups. We found that $V_{c,max25}$ showed a significant phylogenetic signal (Pagel's $\lambda = 0.675$; $p<0.001$) (Fig. 3a). This finding was also supported by the significant differences of $V_{c,max25}$ across the five phylogenetic groups, in which we found that $V_{c,max25}$ increased from the oldest plants (i.e., pteridophyte) to the youngest plants (i.e., monocotyledon) based on the divergence time (Fig. 3b; Table S3). However, while broad differences in $V_{c,max25}$ means certainly existed, $V_{c,max25}$ space was not divided neatly among different phylogenetic groups.

3.3 Relative contribution of environmental factors and evolutionary history to global $V_{c,max25}$ variability

To investigate the relative importance of environmental factors and evolutionary history on shaping global $V_{c,max25}$ variability, we first identified the important environmental factors based on

the model selection, and then conducted a Bayesian phylogenetic linear mixed model to disentangle their separate and joint roles. Seven most important environmental factors were identified to explain a significant proportion of global $V_{c,max25}$ variability: temperature, VPD, elevation, soil silt, soil pH, soil clay, and soil bulk density (Fig. 4). Partial regression analysis indicated that $V_{c,max25}$ decreased significantly with temperature, elevation and soil silt content, but increased with VPD, soil pH, soil clay content and soil bulk density (Fig. 4). After incorporating these seven environmental factors into the Bayesian model, we found that evolutionary history (indicated by phylogeny and species) outweighed the environmental factors in explaining global $V_{c,max25}$ variability, with the current environmental factors as a whole explaining only 18.0% of $V_{c,max25}$ variance, whereas phylogeny and species explained 31.3% and 21.7% of $V_{c,max25}$ variance, respectively (Table 1; Fig. 5). In other words, evolutionary history had nearly three-fold more importance (53.0% vs 18.0%) in explaining the global $V_{c,max25}$ variability than current environmental factors (Fig. 5).

4 Discussion

A deep understanding of the environmental variables and evolutionary history underlying the large-scale $V_{c,max25}$ variability can yield critical insights for the development of TBMs that simulate and forecast terrestrial carbon cycling (Rogers et al., 2017; Walker et al., 2021). However, characterizing the global variability of $V_{c,max25}$ has been challenging, and current approaches provide substantially divergent estimates (Kattge et al., 2009; Ali et al., 2015; Smith & Dukes, 2018). These divergences are likely the result of the poor representativeness of existing datasets of field measured $V_{c,max25}$ that allows us to understand how $V_{c,max25}$ varies spatially, across biomes, and within taxa. We studied the global variability of $V_{c,max25}$ based on an unprecedently large and

geographically comprehensive dataset, with a high degree of variability across Whittaker biomes and life-forms (Fig. 2; Tables S1 and S2). This large variability allowed us to systematically explore biome-specific patterns that were reported based on smaller field-measured datasets. For example, we found higher $V_{c,max25}$ in grasslands relative to shrublands and forests, which was previously reported by Kattge et al. (2009) and Smith et al. (2019). We also found that short-lived, fast-growing species with higher nutrient concentrations and lower leaf mass per area had higher $V_{c,max25}$ than their long-lived, slow-growing counterparts (Fig. 2; Table S2). However, despite significant differences in the mean $V_{c,max25}$, variation within each biome and life-form is too large (Fig. 2; Tables S1 and S2) to allow assigning average $V_{c,max25}$ values for use in TBMs (Rogers et al., 2017) or other practical applications.

So what mechanisms cause such a large variability of $V_{c,max25}$ on a global scale? When the variability explained by phylogeny and species was excluded, we found that the current-day climatic and soil variables altogether explained 18% of this large global $V_{c,max25}$ variability (Table 1). These current environmental conditions can partly explain some of the observed biome-dependent patterns of $V_{c,max25}$. For example, the higher $V_{c,max25}$ in subtropical desert and temperate grassland/desert relative to tropical and temperate rainforests is partly explained by higher VPD, soil pH, and soil bulk density (Table S4). These three environmental variables (i.e., VPD, soil pH and soil bulk density) were picked up in the final statistical model of $V_{c,max25}$ (Fig. 4), and could upregulate $V_{c,max25}$ due to their positive effects on the investments in photosynthetic biochemistry (Maire et al., 2015; Paillassa et al., 2020; Luo et al., 2021; Peng et al., 2021). However, current environmental factors were found to only have a low to moderate accumulative predictive power

on global $V_{c,max25}$ variability (Table 1; Smith et al., 2019; Peng et al., 2021), whereas the evolutionary history could explain much of the remaining variation (Fig. 3; Table 1).

The important role of evolutionary history in explaining global $V_{c,max25}$ variability is particularly evident from two results (its link with phylogenetic structure, and the higher relative weight of evolutionary history over environmental factors). Our results thus unveil the phylogenetic relatedness of $V_{c,max25}$ at global scales, expanding previous results that showed the phylogenetic effect on $V_{c,max25}$ variability at taxon-specific (Huang et al., 2022) and regional scales (Yang et al., 2019; Xu et al., 2021). This phylogenetic structure of $V_{c,max25}$ also adds essential information to the patterns of $V_{c,max25}$ across contrasting biomes with different evolutionary histories. For example, tropical forest biomes are evolutionarily ancient (Ma et al., 2018), while shrubland, woodland, grassland and desert biomes are evolutionarily young (Cavender-Bares et al., 2016; Ma et al., 2018). Such differences in evolutionary history seem to support that most late-emerging ecosystems (e.g. woodland/shrubland, subtropical desert, temperate grassland/desert) have higher $V_{c,max25}$ than the early-emerging ecosystems (e.g. tropical rainforest) (Fig. 2b). In addition, the observed increasing trend of $V_{c,max25}$ in more modern clades is also consistent with the trend of light-saturated photosynthetic rate (A_{max}) over the evolutionary scale (Gago et al., 2019; Flexas & Carriquí, 2020; Huang et al., 2022; Liu et al., 2022). The observed increasing $V_{c,max25}$ and A_{max} along plant phylogeny could possibly be explained by the corresponding variation in the fraction of N_a allocated to RuBisCO, and in leaf structural properties (e.g., mesophyll conductance and cell-wall thickness), which are both tightly related to leaf photosynthesis (Gago et al., 2019; Flexas & Carriquí, 2020; Huang et al., 2022).

We next investigated the relative importance of environmental factors and evolutionary history in explaining global $V_{c,max25}$ variability, and found that evolutionary history (represented by both phylogeny and species) explained a much greater proportion than current environmental factors (Table 1). Phylogeny represents long-term evolution together with ancient adaptation and differentiation from other clades, while species is linked to more recent evolutionary processes, including strong selection within the phylogeny and recent phenotypic/epigenetic shifts that are not directly detectable by phylogenetic information (Sardans et al., 2021; Vallicrosa et al., 2022a,b). Adaptation to different environments in recently separated clades can conduct to a convergent or divergent fast evolution not yet incorporated in the timescales considered in phylogenetic analyses (Sardans et al., 2021). Thus, previous research if only considering the $V_{c,max25}$ control from current-day environmental conditions often results in very small $V_{c,max25}$ variance being explained (Fig. 4; Ali et al., 2015; Smith & Dukes, 2018; Peng et al., 2021). This new paradigm could be applied to other plant traits. For example, studies focusing on multi-elemental concentrations and secondary metabolites also consistently demonstrated the dominant role of evolutionary history in explaining the large-scale variability in various leaf traits (Asner et al., 2014; Sardans et al., 2015, 2021; Palacio et al., 2022; Vallicrosa et al., 2022a,b). Since both evolutionary history information and current environmental factors jointly regulate large-scale variability in plant functional traits, including $V_{c,max25}$, our results further suggest that the variability stored in the species and phylogeny must be credited, in addition to the site associated current environmental factors, to accurately estimate and project the global $V_{c,max25}$ variability. However, it should be noted that the exclusion of species within clades may have major effects on the interpretation of the evolutionary history in shaping $V_{c,max25}$ variability, which should merit further study with a larger dataset including enough data coverage within clades.

In summary, this study firstly revealed that $V_{c,max25}$ showed significant biogeographical patterns at global scale, and varied remarkably within and across different biomes and life-forms. Secondly, $V_{c,max25}$ exhibited a significant phylogenetic signal with the evolution trend towards higher values in more modern clades. Thirdly, evolutionary history consisted of both phylogeny and species largely outperformed current-day environmental conditions in explaining global $V_{c,max25}$ variability. These results collectively suggest that dynamics related to evolutionary history could be first-order priorities for improving theoretical understanding and modelling of global $V_{c,max25}$ variability. In addition to the effects of evolutionary history and environmental factors that cumulatively explained 71% of the total variance, there remained a considerable proportion (29%) of unexplained $V_{c,max25}$ variability. Some of this unexplained $V_{c,max25}$ variability could be attributed to phenological variability in measuring young and old leaves (Albert et al., 2018; Wu et al., 2019), the random measurement and sampling error in our assembled $V_{c,max25}$ records (Bloomfield et al., 2018), other unexplored but important environmental factors (e.g. day length, soil moisture, soil available phosphorus concentration) (Ali et al., 2015; Maire et al., 2015; Smith & Dukes, 2018), and intraspecific variability at a single site (Bloomfield et al., 2018; Sardans et al., 2021). These warrant more sophisticated investigation through experimental manipulation and field observation approaches across large environmental gradients.

With these results, our work generates at least two insights for mechanistic understanding of global $V_{c,max25}$ variability and terrestrial biosphere modelling. First, our finding can complement current understandings of fundamental controls on global $V_{c,max25}$ variability. Most previous studies only considered the effects of current-day environmental conditions (Kattge et al., 2009; Ali et al., 2016;

Smith et al., 2019; Peng et al., 2021) and failed to account for evolutionary history, which displayed nearly three-fold higher contribution than current-day environmental factors. Our identified three major factors (i.e., current environment factors, phylogeny and species) for $V_{c,max25}$ further lends us with a hypothesized time-scale dependent processes in regulating global $V_{c,max25}$ variability, thus providing a novel mechanistic framework for characterizing the variability of $V_{c,max25}$ and, resultingly, plant photosynthesis across large geographical extents (Rogers et al., 2017). Given that the evolutionary divergence within the same clade or the rate of evolutionary convergence among species from different clades could be increased by recent evolutionary pressures (e.g. climate warming, species migration and shifts in species interactions; Puurtinen et al., 2016; Molina-Montenegro et al., 2018), our finding further implies that global changes may restructure $V_{c,max25}$ biogeography through not only the plastic responses via the direct and short-term environmental effects, but also the changes in species and phylogenetic distributions.

Second, our findings also shed critical insights for future work aiming to model $V_{c,max25}$ variability. The dominant role of evolutionary history in shaping global $V_{c,max25}$ variability provides an important benchmark and theoretical basis for evaluating current $V_{c,max25}$ models, including optimality models based on eco-evolutionary first-principles (Wang et al., 2017; Smith et al., 2019). Future studies should explore potential ways to mechanistically incorporate evolutionary history information into the theoretical modelling of $V_{c,max25}$ and thus better constrain TBMs to improve simulations of terrestrial photosynthesis, carbon cycling and climate change responses (Bonan & Doney, 2018; Walker et al., 2021). This could be helped by leveraging other datasets and models for model integration and benchmarking, such as the Global Biodiversity Information Facility (GBIF) occurrences with globally georeferenced species data, Species Distribution Models (SDMs;

Elith & Leathwick, 2009), and the species classification capacity of remotely sensed imaging spectroscopy and laser imaging detection and ranging (LiDAR) techniques (Cavender-Bares et al., 2020). While challenging, our results indicate that facilitating the inclusion of species and phylogenetic information in large-scale models is greatly needed in the future.

References

Albert, L. P., Wu, J., Prohaska, N., Camargo, P. B., Huxman, T. E., Tribuzy, E. S., Ivanov, V. Y., Oliveira, R. S, Garcia, S., Smith, M. N., Oliveira Junior, R. C., Restrepo-Coupe, N., da Silva, R., Stark, S. C, Martins, G. A., Penha, D. V., & Saleska, S. R. (2018). Age-dependent leaf physiology and consequences for crown-scale carbon uptake during the dry season in an Amazon evergreen forest. *New Phytologist*, *219,* 870-884.

Ali, A. A., Xu, C. G., Rogers, A., McDowell, N. G., Medlyn, B. E., Fisher, R. A., Wullschleger, S. D., Reich, P. B., Vrugt, J. A., Bauerle, W. L., Santiago, L. S., & Wilson, C. J. (2015). Global-scale environmental control of plant photosynthetic capacity. *Ecological Applications*, *25,* 2349-2365.

Ali, A. A., Xu, C. G., Rogers, A., Fisher, R. A., Wullschleger, S. D., Massoud, E. C., Vrugt, J. A., Muss, J. D., McDowell, N. G., Fisher, J. B., Reich, P. B., & Wilson, C. J. (2016). A global scale mechanistic model of photosynthetic capacity (LUNA V1. 0). *Geoscientific Model Development*, *9*, 587-606.

Atkin, O. K., Bloomfield, K. J., Reich, P. B., Tjoelker, M.G., Asner, G. P., Bonal, D., Bonisch, G., Bradford, M. G., Cernusak, L. A., Cosio, E. G., Creek, D., Crous, K. Y., Domingues, T. F., Dukes, J. S., Egerton, J. J., Evans, J. R., Farquhar, G. D., Fyllas, N. M., Gauthier, P. P.,

… Zaragoza-Castells, J. (2015). Global variability in leaf respiration in relation to climate, plant functional types and leaf traits. *New Phytologist, 206,* 614-636.

Asner, G. P., Martin, R. E., Tupayachi, R., Anderson, C. B., Sinca, F., Carranza-Jiménez, L., & Martinez, P. (2014). Amazonian functional diversity from forest canopy chemical assembly. *Proceedings of the National Academy of Sciences, USA, 111,* 5604-5609.

Bahar, N. H. A., Ishida, F. Y., Weerasinghe, L. K., Guerrieri, R., O'Sullivan, O. S., Bloomfield, K. J., Asner, G. P., Martin, R. E., Lloyd, J., Malhi, Y., Phillips, O. L., Meir, P., Salinas, N., Cosio, E. G., Domingues, T. F., Quesada, C. A., Sinca, F., Escudero Vega, A., Zuloaga Ccorimanya, P. P., … Atkin, O. K. (2017). Leaf-level photosynthetic capacity in lowland Amazonian and high-elevation Andean tropical moist forests of Peru. *New Phytologist, 214,* 1002-1018.

Bernacchi, C. J., Bagley, J. E., Serbin, S. P., Ruiz-Vera, U. M., Rosenthal, D. M., & Vanloocke, A. (2013). Modelling C_3 photosynthesis from the chloroplast to the ecosystem. *Plant Cell & Environment, 36,* 1641-1657.

Bloomfield, K. J., Cernusak, L. A., Eamus, D., Ellsworth, D. S., Prentice, I. C., Wright, I. J., Boer, M. M., Bradford, M. G., Cale, P., Cleverly, J., Egerton, J. J. G., Evans, B. J., Hayes, L. S., Hutchinson, M. F., Liddell, M. J., Macfarlane, C., Meyer, W. S., Prober, S. M., Togashi, H. F., … Atkin, O. K. (2018). A continental-scale assessment of variability in leaf traits: Within species, across sites and between seasons. *Functional Ecology, 32,* 1492-1506.

Bonan, G. B., & Doney, S. C. (2018). Climate, ecosystems, and planetary futures: the challenge to predict life in Earth system models. *Science, 359,* eaam8328.

Bracher, A., Whitney, S. M., Hartl, F. U., & Hayer-Hartl, M. (2017). Biogenesis and metabolic maintenance of Rubisco. *Annual Review of Plant Biology, 68,* 29-60.

Breheny, P., & Burchett, W. (2017). Visualization of regression models using visreg. R journal, *9*, 56-71.

Calcagno, V., & de Mazancourt, C. (2010). glmulti: an R package for easy automated model selection with (generalized) linear models. *Journal of Statistical Software*, *34*, 1-29.Cavender-Bares, J., Ackerly, D. D., Hobbie, S. E., & Townsend, P. A. (2016). Evolutionary legacy effects on ecosystems: Biogeographic origins, plant traits, and implications for management in the era of global change. *Annual Review of Ecology, Evolution, and Systematics*, *47*, 433-462.

Cavender-Bares, J., Gamon, J. A., & Townsend, P. A. (2020). *Remote sensing of plant biodiversity*. Springer Nature.

Cernusak, L. A., Hutley, L. B., Beringer, J., Holtum, J. A. M., & Turner, B. L. (2011). Photosynthetic physiology of eucalypts along a sub-continental rainfall gradient in northern Australia. *Agricultural and Forest Meteorology*, *151*, 1462-1470.

Dahlin, K. M., Asner, G. P., & Field, C. B. (2013). Environmental and community controls on plant canopy chemistry in a Mediterranean-type ecosystem. *Proceedings of the National Academy of Sciences, USA*, *110*, 6895-6900.

Davis, T. W., Prentice, I. C., Stocker, B. D., Thomas, R. T., Whitley, R. J., Wang, H., Evans, B. J., Gallego-Sala, A. V., Sykes, M. T., & Cramer, W. (2017). Simple process-led algorithms for simulating habitats (SPLASH v.1.0): Robust indices of radiation, evapotranspiration and plant-available moisture. *Geoscientific Model Development*, *10*, 689-708.

Detto, M., & Xu, X. (2020). Optimal leaf life strategies determine $V_{c,max}$ dynamic during ontogeny. *New Phytologist*, *228*, 361-375.

517 Domingues, T. F., Meir, P., Feldpausch, T. R., Saiz, G., Veenendaal, E. M., Schrodt, F., Bird, M.,
518 Djagbletey, G., Hien, F., Compaore, H., Diallo, A., Grace, J., & Lloyd, J. (2010). Co-
519 limitation of photosynthetic capacity by nitrogen and phosphorus in West Africa
520 woodlands. *Plant Cell & Environment*, *33*, 959-980.
521 Domingues, T. F., Ishida, F. Y., Feldpausch, T. R., Grace, J., Meir, P., Saiz, G., Sene, O., Schrodt,
522 F., Sonké, B., Taedoumg, H., Veenendaal, E. M., Lewis, S., & Lloyd, J. (2015). Biome-
523 specific effects of nitrogen and phosphorus on the photosynthetic characteristics of trees at
524 a forest-savanna boundary in Cameroon. *Oecologia*, *178*, 659-672.
525 Doetterl, S., Stevens, A., Six, J., Merckx, R., Van Oost, K., Casanova Pinto, M., Casanova-Katny,
526 A., Muñoz, C., Boudin, M., Zagal Venegas, E., & Boeckx, P. (2015). Soil carbon storage
527 controlled by interactions between geochemistry and climate. *Nature Geoscience*, *8*, 780-
528 783.
529 Dong, N., Prentice, I. C., Evans, B. J., Caddy-Retalic, S., Lowe, A. J., & Wright, I. J. (2017). Leaf
530 nitrogen from first principles: field evidence for adaptive variation with climate.
531 *Biogeosciences*, *14*, 481-495.
532 Du, E. Z., Terrer, C., Pellegrini, A. F. A., Ahlström, A., van Lissa, C. J., Zhao, X., Xia, N., Wu, X.
533 H., & Jackson, R. B. (2020). Global patterns of terrestrial nitrogen and phosphorus
534 limitation. *Nature Geoscience*, *13*, 221-226.
535 Elith, J., & Leathwick, J. R. (2009). Species distribution models: ecological explanation and
536 prediction across space and time. *Annual Review of Ecology, Evolution, and Systematics*,
537 *40*, 677-697.
538 Farquhar, G. D., von Caemmerer, S., & Berry, J. A. (1980). A biochemical model of photosynthetic
539 CO_2 assimilation in leaves of C_3 species. *Planta*, *149*, 78-90.

Felsenstein, J. (1985). Phylogenies and the comparative method. *The American Naturalist*, *125*, 1-15.

Flexas, J., & Carriquí, M. (2020). Photosynthesis and photosynthetic efficiencies along the terrestrial plant's phylogeny: lessons for improving crop photosynthesis. *The Plant Journal*, *101*, 964-978.

Gago, J., Carriquí, M., Nadal, M., Clemente-Moreno, M. J., Coopman, R. E., Fernie, A. R., & Flexas, J. (2019). Photosynthesis optimized across land plant phylogeny. *Trends in Plant Science*, *24*, 947-958.

Galmes, J., Kapralov, M. V., Copolovici, L. O., Hermida-Carrera, C., & Niinemets, Ü. (2015). Temperature responses of the Rubisco maximum carboxylase activity across domains of life: phylogenetic signals, trade-offs, and importance for carbon gain. *Photosynthesis research*, *123*, 183-201.

Han, W. X., Fang, J. Y., Guo, D. L., & Zhang, Y. (2005). Leaf nitrogen and phosphorus stoichiometry across 753 terrestrial plant species in China. *New Phytologist*, 168: 377-385.

Harris, I., Jones, P. D., Osborn, T. J., & Lister, D. H. (2014). Updated high resolution grids of monthly climatic observations-the CRU TS3.10 Dataset. *International journal of climatology*, *34*, 623-642.

Huang, G. J., Peng, S. B., & Li, Y. (2022). Variation of photosynthesis during plant evolution and domestication: implications for improving crop photosynthesis. *Journal of Experimental Botany*, *73*, 4886-4896.

Jiang, C., Ryu, Y., Wang, H., & Keenan, T. F. (2020). An optimality-based model explains seasonal variation in C_3 plant photosynthetic capacity. *Global Change Biology*, *26*, 6493-6510.

Jin, Y., & Qian, H. (2019). V.PhyloMaker: an R package that can generate very large phylogenies for vascular plants. *Ecography*, *42*, 1353-1359.

Jump, A. S., & Peñuelas, J. (2005). Running to stand still: adaptation and the response of plants to rapid climate change. *Ecology Letters*, *8*, 1010-1020.

Kattge, J., & Knorr, W. (2007). Temperature acclimation in a biochemical model of photosynthesis: a reanalysis of data from 36 species. *Plant, Cell & Environment*, *30*, 1176-1190.

Kattge, J., Knorr, W., Raddatz, T., & Wirth, C. (2009). Quantifying photosynthetic capacity and its relationship to leaf nitrogen content for global-scale terrestrial biosphere models. *Global Change Biology*, *15*, 976-991.

Liu, H., Ye, Q., Simpson, K. J., Cui, E. Q., & Xia, J. Y. (2022). Can evolutionary history predict plant plastic responses to climate change? *New Phytologist*, *235*, 1260-1271.

Luo, X. Z., Keenan, T. F., Chen, J. M., Croft, H., Prentice, C. I., Smith, N. G., Walker, A. P., Wang, H., Wang, R., Xu, C. G., & Zhang, Y. (2021). Global variation in the fraction of leaf nitrogen allocated to photosynthesis. *Nature communications*, *12*, 1-10.

Ma, Z. Q., Guo, D. L., Xu, X. L., Lu, M. Z., Bardgett, R. D., Eissenstat, D. M., McCormack, M. L., & Hedin, L. O., (2018). Evolutionary history resolves global organization of root functional traits. *Nature*, *555*, 94-97.

Maire, V., Wright, I. J., Prentice, I. C., Batjes, N. H., Bhaskar, R., Bodegom, P. M., Cornwell, W. K, Ellsworth, D., Niinemets, Ü., Ordonez, A., Reich, P. B., & Santiago, L. S. (2015). Global effects of soil and climate on leaf photosynthetic traits and rates. *Global Ecology and Biogeography*, *24*, 706-717.

Meir, P., Levy, P. E., Grace, J., & Jarvis, P. G. (2007). Photosynthetic parameters from two contrasting woody vegetation types in West Africa. *Plant Ecology*, *192*, 277-287.

Molina-Montenegro, M. A., Acuña-Rodríguez, I. S., Flores, T. S. M., Hereme, R., Lafon, A., Atala, C., & Torres-Díaz, C. (2018). Is the causes of plant invasions the result of rapid adaptive evolution in seed traits? Evidence a latitudinal rainfall gradient? *Frontiers in Plant Science*, *9*, 208.

Münkemüller, T., Lavergne, S., Bzeznik, B., Dray, S., Jombart, T., Schiffers, K., & Thuiller, W. (2012). How to measure and test phylogenetic signal. *Methods in Ecology and Evolution*, *3*, 743-756.

Paillassa, J., Wright, I. J., Prentice, I. C., Pepin, S., Smith, N. G., Ethier, G., Westerband, A. C., Lamarque, L. J., Wang, H., Cornwell, W. K., & Maire, V. (2020). When and where soil is important to modify the carbon and water economy of leaves. *New Phytologist*, *228*, 121-135.

Palacio, S., Cera, A., Escudero, A., Luzuriaga, A.L., Sánchez, A. M., Mota, J. F., Perez-Serrano S. M., Merlo, M. E., Martinez-Hernandez, F., Salmeron-Sanchez, E., Mendoza-Fernandez, A. J., Perez-Garcia, F. J., Montserrat-Marti, G., & Tejero, P. (2022). Recent and ancient evolutionary events shaped plant elemental composition of edaphic endemics. A phylogeny-wide analysis of Iberian gypsum plants. *New Phytologist*, *235*, 2406-2423.

Peng, Y. K., Bloomfield, K. J., Cernusak, L. A., Domingues, T. F., & Prentice, I. C. (2021). Global climate and nutrient controls of photosynthetic capacity. *Communications Biology*, *4*, 462.

Peñuelas, J., Fernández-Martínez, M., Ciais, P., Jou, D., Piao, S., Obersteiner, M., Vicca, S., Janssens, I. A., & Sardans, J. (2019). The bioelements, the elementome, and the biogeochemical niche. *Ecology*, *100*, e02652.

Prentice, I. C., Dong, N., Gleason, S. M., Maire, V., & Wright, I. J. (2014). Balancing the costs of carbon gain and water transport: testing a new theoretical framework for plant functional ecology. *Ecology Letters*, *17*, 82-91.

Puurtinen, M., Elo, M., Jalasvuori, M., Kahilainen, A., Ketola, T., Kotiaho, J. S., Mönkkönen, M., & Pentikäinen, O. T. (2016). Temperature-dependent mutational robustness can explain faster molecular evolution at warm temperatures, affecting speciation rate and global patterns of species diversity. *Ecography*, *39*, 1025-1033.

Revell, L. J. (2012). Phytools: an R package for phylogenetic comparative biology (and other things). *Methods in Ecology and Evolution*, *3*, 217-223.

Rogers, A., Medlyn, B. E., Dukes, J. S., Bonan, G., Caemmerer, S., Dietze, M. C., Kattge, J, Leakey, A. D. B., Mercado, L. M., Niinemets, Ü., Prentice, I. C., Serbin, S. P., Sitch, S., Way, D. A., & Zaehle, S. (2017). A roadmap for improving the representation of photosynthesis in Earth system models. *New Phytologist*, *213*, 22-42.

Sardans, J., Janssens, I. A., Alonso, R., Veresoglou, S. D., Rillig, M. C., Sanders, T. G., Carnicer, J., Filella, I., Farré-Armengol, G, & Peñuelas, J. (2015). Foliar elemental composition of European forest tree species associated with evolutionary traits and present environmental and competitive conditions. *Global Ecology and Biogeography*, *24*, 240-255.

Sardans, J., Vallicrosa, H., Zuccarini, P., Farré-Armengol, G., Fernández-Martínez, M., Peguero, G., Gargallo-Garriga, A., Ciais, P., Janssens, I. A., Obersteiner, M., Richter, A., & Penuelas, J. (2021). Empirical support for the biogeochemical niche hypothesis in forest trees. *Nature Ecology & Evolution*, *5*, 184-194.

Smith, N.G., & Dukes, J.S. (2017). LCE: Leaf carbon exchange dataset for tropical, temperate, and boreal species of North and Central America. *Ecology*, *98*, 2978.

630 Smith, N.G., & Dukes, J.S. (2018). Drivers of leaf carbon exchange capacity across biomes at the
631 continental scale. *Ecology*, *99*, 1610-1620.
632 Smith, N.G., Keenan, T.F., Prentice, I.C., Wang, H., Wright, I.J., Niinemets, Ü., Crous, K. Y.,
633 Domingues, T. F., Guerrieri R., Yoko Ishida, F., Kattge, J., Kruger, E. L., Maire, V., Rogers,
634 A., Serbin, S. P., Tarvainen, L., Togashi, H. F., Townsend, P. A., Wang, M., … Zhou, S.
635 X. (2019). Global photosynthetic capacity is optimized to the environment. *Ecology Letters*,
636 *22*, 506-517.
637 Vallicrosa, H., Sardans, J., Maspons, J., Zuccarini, P., Fernández-Martínez, M., Bauters, M., Goll,
638 D. S., Ciais, P., Obersteiner, M., Janssens, I. A., & Penuelas, J. (2022a). Global maps and
639 factors driving forest foliar elemental composition: The importance of evolutionary history.
640 *New Phytologist*, *233*, 169-181.
641 Vallicrosa, H., Sardans, J., Maspons, J., & Peñuelas, J. (2022b). Global distribution and drivers of
642 forest biome foliar nitrogen to phosphorus ratios (N:P). *Global Ecology and Biogeography*,
643 *31*, 861-871.
644 Walker, A. P., Beckerman, A. P., Gu, L. H., Kattge, J., Cernusak, L. A., Domingues, T. F., Scales,
645 J. C., Wohlfahrt, G., Wullschleger, S. D., & Woodward, F. I. (2014). The relationship of
646 leaf photosynthetic traits-V_{cmax} and J_{max} to leaf nitrogen, leaf phosphorus, and specific leaf
647 area: a meta-analysis and modeling study. *Ecology and Evolution*, *4*, 3218-3235.
648 Walker, A. P., De Kauwe, M. G., Bastos, A., Belmecheri, S., Georgiou, K., Keeling, R. F.,
649 McMahon, S. M., Medlyn, B. E., Moore, D. J. P., Norby, R. J, Zaehle, S., Anderson-
650 Teixeira, K. J., Battipaglia, G., Brienen, R. J. W., Cabugao, K. G., Cailleret, M., Campbell,
651 E., Canadell, J. G., Ciais, P., … Zuidema, P. A. (2021). Integrating the evidence for a

terrestrial carbon sink caused by increasing atmospheric CO_2. *New Phytologist*, *229*, 2413-2445.

Wang, H., Prentice, I. C., Keenan, T. F., Davis, T. W., Wright, I. J., Cornwell, W. K., Evans, B. J., & Peng, C. H. (2017). Towards a universal model for carbon dioxide uptake by plants. *Nature Plants*, *3*, 734-741.

Wang, H., Harrison, S. P., Prentice, I. C., Yang, Y. Z., Bai, F., Togashi, H. F., Wang, M., Zhou, S. X., & Ni, J. (2018). The China Plant Trait Database: towards a comprehensive regional compilation of functional traits for land plants. *Ecology*, *99*, 500-500.

Wang, H., Atkin, O. K., Keenan, T. F., Smith, N. G., Wright, I. J., Bloomfield, K. J., Kattge, J., Reich, P. B., & Prentice, I. C. (2020). Acclimation of leaf respiration consistent with optimal photosynthetic capacity. *Global Change Biology*, *26*, 2573-2583.

Weedon, G. P., Balsamo, G., Bellouin, N., Gomes, S., Best, M. J., & Viterbo, P. (2014). The WFDEI meteorological forcing data set: WATCH Forcing Data methodology applied to ERA-Interim reanalysis data. *Water Resource Research*, *50*, 7505-7514.

Whittaker, R. H. (1975). *Communities and Ecosystems*. (MacMillan), pp. 385.

Wright, I. J., Reich, P. B., Westoby, M., Ackerly, D. D., Baruch, Z., Bongers, F., Cavender-Bares, J., Chapin, T., Cornelissen, J. H. C., Diemer, M., Flexas, J., Garnier, E., Groom, P. K., Gulias, J., Hikosaka, K., Lamont, B. B., Lee, T., Lee, W., Lusk, C., … Villar, R. (2004). The worldwide leaf economics spectrum. *Nature*, *428*, 821-827.

Wu, J., Albert, L. P., Lopes, A. P., Restrepo-Coupe, N., Hayek, M., Wiedemann, K. T., Guan, K. Y., Stark, S. C., Christoffersen B., Prohaska, N., Tavares, J. V., Marostica, S., Kobayashi, H., Ferreira, M. L., Campos, K. S., da Silva, R., Brando, P. M., Dye, D. G., Huxman, T.

E., … Saleska, S. R. (2016). Leaf development and demography explain photosynthetic seasonality in Amazon evergreen forests. *Science, 351*, 972-976.

Wu, J., Rogers, A., Albert, L. P., Ely, K., Prohaska, N., Wolfe, B. T., Oliveira Jr, R. C., Saleska, S. R., & Serbin, S. P. (2019). Leaf reflectance spectroscopy captures variation in carboxylation capacity across species, canopy environment and leaf age in lowland moist tropical forests. *New Phytologist*, *224*, 663-674.

Xu, H. Y., Wang, H., Prentice, I. C., Harrison, S. P., & Wright, I. J. (2021). Coordination of plant hydraulic and photosynthetic traits: confronting optimality theory with field measurements. *New Phytologist*, *232*, 1286-1296.

Yan, Z. B., Guo, Z. F., Serbin, S. P., Song, G. Q., Zhao, Y. Y., Chen, Y., Wu, S. B., Wang, J., Wang, X., Li, J., Wang, B., Wu, Y., Su, Y., Wang, H., Rogers, A., Liu, L. L., & Wu, J. (2021). Spectroscopy outperforms leaf trait relationships for predicting photosynthetic capacity across different forest types. *New Phytologist*, *232*, 134-147.

Yang, Y. Z., Wang, H., Harrison, S. P., Prentice, I. C., Wright, I. J., Peng, C. H., & Lin, G. H. (2019). Quantifying leaf-trait covariation and its controls across climates and biomes. *New Phytologist*, *221*, 155-168.

Zhang, J. H., He, N. P., Liu, C. C., Xu, L., Chen, Z., Li, Y., Wang, R. M., Yu, G. R., Sun, W., Xiao, C. W., Chen, H. Y. H., & Reich, P. B. (2020). Variation and evolution of C:N ratio among different organs enable plants to adapt to N-limited environments. *Global Change Biology*, *26*, 2534-2543.

Data Availability Statement

All data used in our study will be uploaded to the Dryad Digital Repository after the manuscript is accepted.

Conflict of Interest

The authors declare no competing interests.

Supporting information

Additional Supporting Information may be found online in the Supporting Information section.

TABLE 1 Results from Bayesian phylogenetic linear mixed model of $V_{c,max25}$ at site-species level with fixed factors (i.e., environmental factors) and random factors (i.e., phylogeny+species) taking into account. The site-species level was analyzed by using the averaged $V_{c,max25}$ for each species within the same sampling site. R^2_c= Percentage of variance explained by all the model (fixed + random). R^2_m= Percentage of variance explained by fixed factors. R^2_p = Percentage of variance explained by phylogeny. R^2_s=Percentage of variance explained by species. Abbreviations: T, mean growing-season temperature; VPD, vapor pressure deficit; Silt, soil silt content; pH, soil pH; Clay, soil clay content; BD, soil bulk density.

Bayesian model	The statistics of fixed variables						Model statistics
$V_{c,max25}$ ~ T + VPD + Elevation + Silt + pH + Clay + BD + (random=phylogeny + species)		post.mean	lower 95% CI	upper 95% CI	eff.samp	pMCMC	R^2_m = 0.180 R^2_c = 0.710 R^2_p = 0.313 R^2_s = 0.217
	Intercept	-1.1078	-1.6765	-0.4602	1700	0.0012	
	T	-0.0732	-0.0840	-0.0622	1700	<0.0001	
	VPD	0.6207	0.4619	0.8081	1444	<0.0001	
	Elevation	-0.0003	-0.0004	-0.0002	1817	<0.0001	
	Silt	-0.0134	-0.0167	-0.0100	1700	<0.0001	
	pH	0.2105	0.1557	0.2606	1700	<0.0001	
	Clay	0.0182	0.0145	0.0222	1962	<0.0001	
	BD	0.5682	0.2791	0.8530	1700	<0.0001	

FIGURE 1 Site distribution of the newly compiled field-measured $V_{c,max}$ dataset (n=6917 records from 425 sites) for C_3 plants worldwide. (a) Location of each sampling site in a background of world map. The points with different color and size indicate the sites with different numbers of observations. (b) Location of each sampling site superimposed upon classic Whittaker Biome Classification by climate.

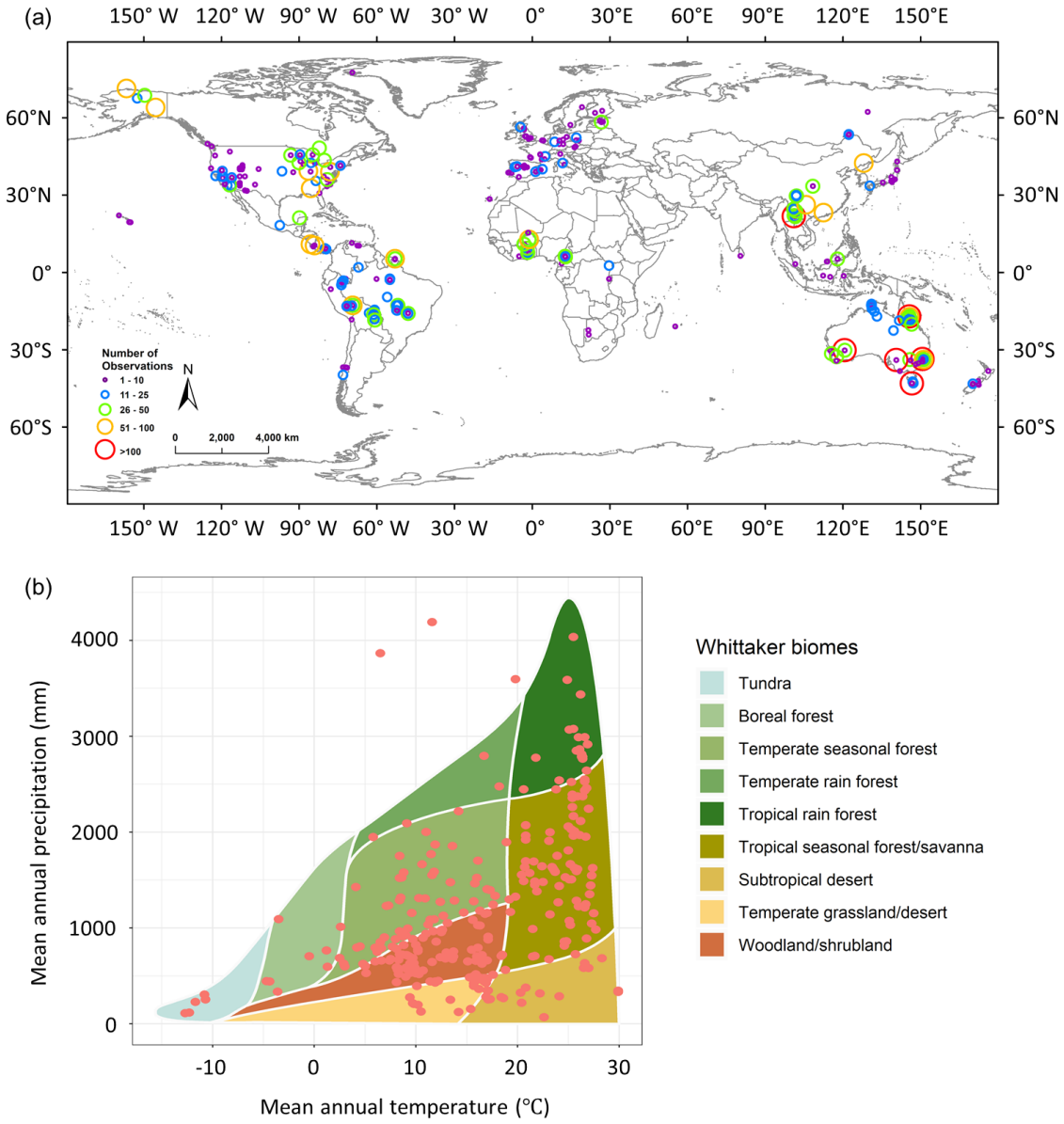

FIGURE 2 Patterns of $V_{c,max25}$ across different Whittaker biomes (a) and life-forms (b-g). The white circles and the boxes within each violin plot show the mean values and the 95% confidence intervals, and the whiskers in each violin plot represent the range. Different lower-case letters adjoining the violin plots indicate significant difference (p<0.05) among different groups for the log transformed $V_{c,max25}$ based on one-way analysis of variance with the least significant difference post-hoc test. The patterns of $V_{c,max25}$ across different biomes and life-forms were analysed at the site-species (i.e., the averaged $V_{c,max25}$ for each species within the same sampling site) and species levels (i.e., the averaged $V_{c,max25}$ for each species), respectively. The number above each violin plot in panel (a) is the number of records for the site-species combinations within that group; and the number above each violin plot in panel (b-g) is the number of species within that group.

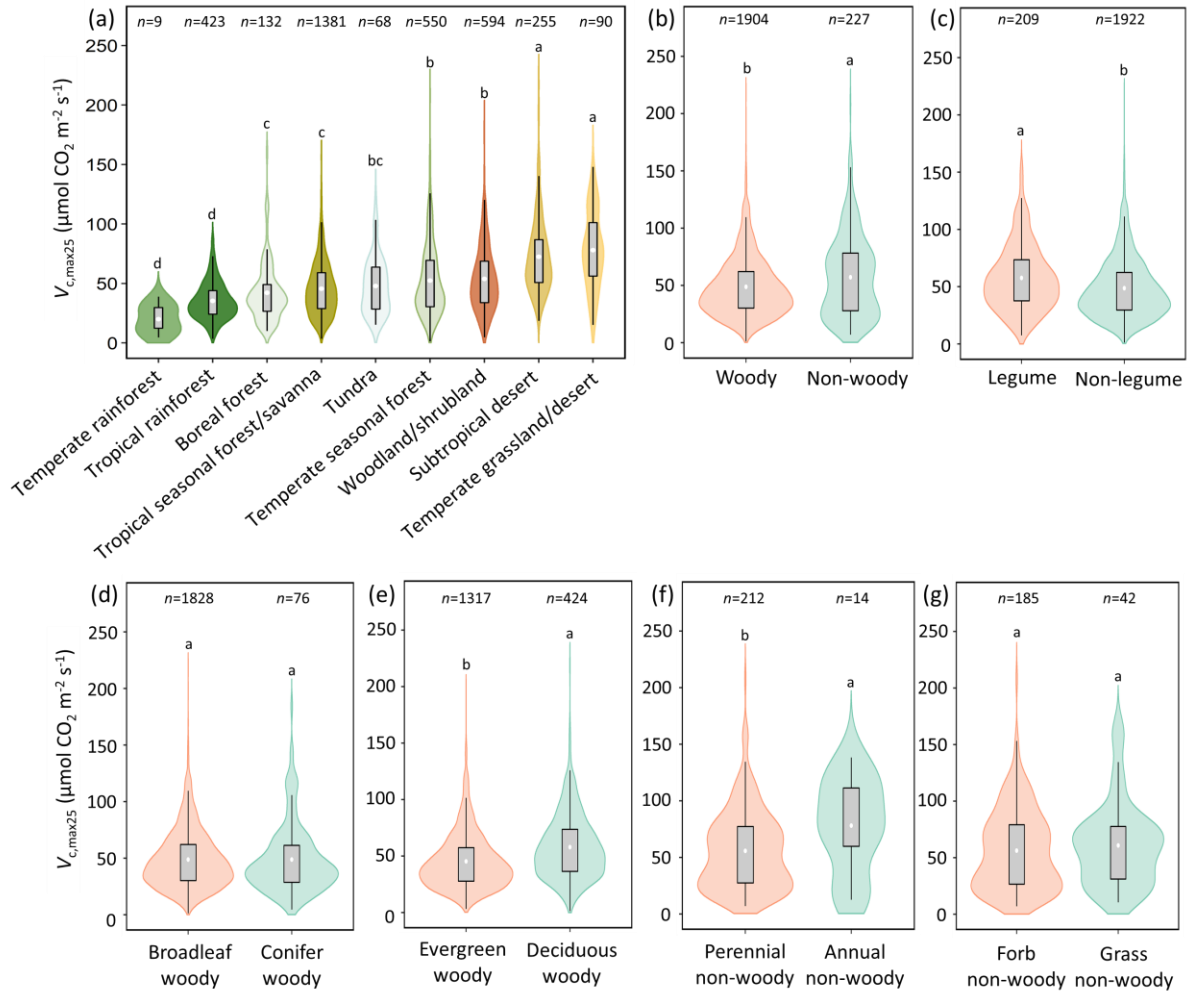

FIGURE 3 Phylogenetic structure of global $V_{c,max25}$ variability. (a) Phylogenetic tree of the 2157 species and the phylogenetic signal of $V_{c,max25}$ indicated by the statistic metric of Pagel's λ. (b) Change in $V_{c,max25}$ across different phylogenetic groups. The white circles and the boxes within each violin plot show the mean values and the 95% confidence intervals, and the whiskers in each violin plot represent the range. Different lower-case letters adjoining the violin plots indicate significant difference (p<0.05) among different groups for the log transformed $V_{c,max25}$ based on one-way analysis of variance with the least significant difference post-hoc test. The number above each violin plot is the number of species within that group.

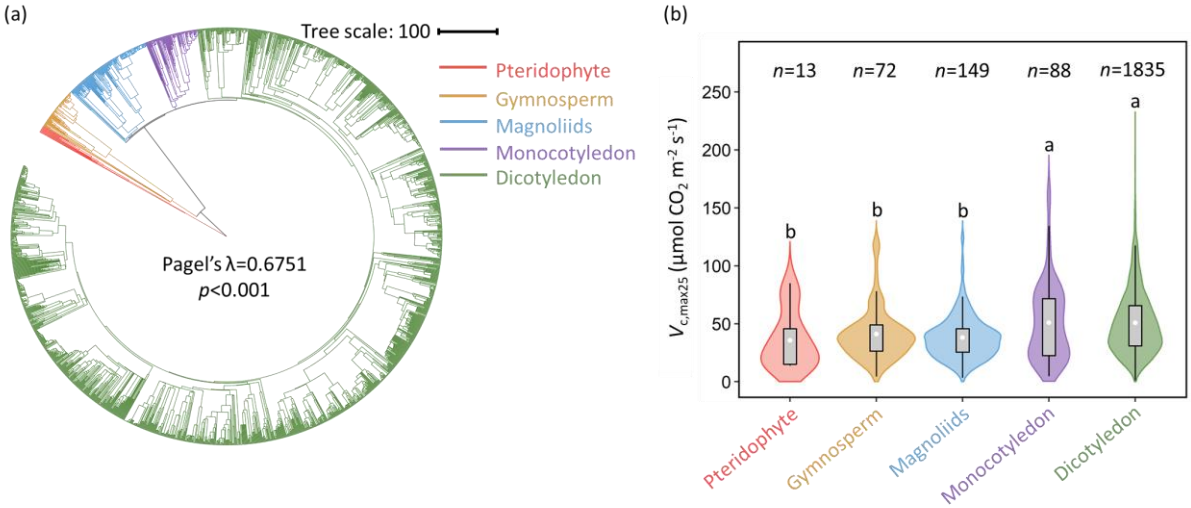

FIGURE 4 Relative importance of environmental factors in predicting global $V_{c,max25}$ variability. (a) The relative importance of each variable is based on the sum of the Akaike weights derived from a model selection using the corrected Akaike Information Criterion (AICc); (b-h) partial regression plots of $V_{c,max25}$ with the predictor of mean growing-season temperature, vapor pressure deficit (VPD), elevation, soil silt content, soil pH, soil clay content, and soil bulk density, respectively. The cutoff (dashed line) of panel (a) is set at 0.8 for identifying the most important predictor variables; the shade areas in (b-h) are 95% confidential intervals around the predicted relationships. Environmental factors include six aboveground environmental factors (i.e., temperature, VPD, incoming photosynthetically active radiation (PAR), precipitation, atmosphere CO_2 concentration (C_a) and elevation) and eight soil variables (i.e., pH, ratio of actual evapotranspiration to equilibrium evapotranspiration (α), clay content, silt content, N content, C:N ratio, bulk density, and cation exchange capacity (CEC)).

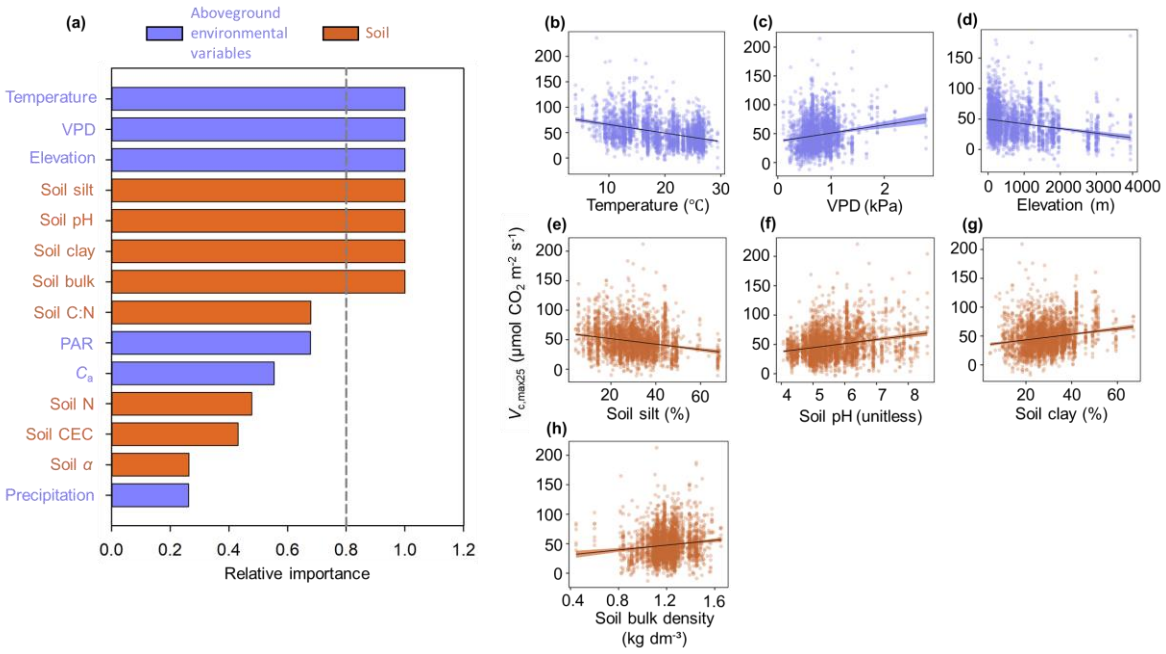

FIGURE 5 Percentage of variance explained by environmental factors and evolutionary history (represented by both phylogeny and species). R^2_m=Percentage of variance explained by the seven important environmental factors (Fig. 4). R^2_p=Percentage of variance explained by phylogeny. R^2_s=Percentage of variance explained by species. R^2_c=Percentage of variance explained by both environmental factors and evolutionary history. Bayesian phylogenetic linear mixed model was used to disentangle the role of different factors in shaping global $V_{c,max25}$ variability (Table 1).